APPENDIX

Appendix A Conference

1. **Kunchit Singsoog**, Panida Pilasuta, Supasit Paengson, Wanachaporn Namhongsa, Weerasak Charoenrat, Surasak Ruamruk, Wiruj Impho, Phanuwat Wongsangnoi, Wasana Kasemsin, Tosawat Seetawan, "The Effect of Silver and Bisnuth doped Mg_2Si on Crystal Structure and Thermoelectric Properties, ***The 4th Southeast Asia Conference on Thermoelectrics***, December 15-18, 2016, Sea Garden Hotel, Danang, Vietnam
2. **K. Singsoog**, P. Pilasuta, S. Paengson, W. Namhongsa, W. Charoenrat, S. Ruamruk, P. Wongsangnoi, W. Impho, W. Kasemsin, and T. Seetawan, The Effect of Temperature Sintering on Thermoelectric Property of Higher Manganese Silicide, ***3th International Conference on Applied Physics and Material Applications (ICAPMA2017)***, 28-29 May 2017, Suan Sunandha Rajabhat University, Bangkok, Thailand
3. **Kunchit Singsoog** and Tosawat Seetawan, Power Generation of p-$MnSi_{1.75}$ and n-Ag doped Mg_2Si Module, ***Innovation for the Advancement and Competitiveness of the Nation (ISSIMM2017)***, 25-26 August 2017, Surabaya, Indonesia
4. **K. Singsoog**, P. Pilasuta, S. Paengson, W. Namhongsa, S. Ruamruk, T. Seetawan, Finite Element Simulations of n-Mg_2Si and p-$MnSi_{1.75}$ Thermoelectric Generator, 31st October – 3rd November 2017, The Empress Hotel, Chiang Mai, Thailand

Appendix B Publications

1. **Kunchit Singsoog**, Panida Pilasuta, Supasit Paengson, Wanachaporn Namhongsa, Weerasak Charoenrat, Surasak Ruamruk, Wiruj Impho, Phanuwat Wongsangnoi, Wasana Kasemsin, Tosawat Seetawan, "The Effect of Silver and Bisnuth doped Mg_2Si on Crystal Structure and Thermoelectric Properties", ***Journal of Materials Science and Applied Energy.*** 6(1), (2017) pp. 102-105 (ACI)
2. **Kunchit Singsoog**, Panida Pilasuta, Supasit Paengson, Wanachaporn Namhongsa, Weerasak Charoenrat, Surasak Ruamruk, Phanuwat Wongsangnoi, Wiruj Impho, Wasana Kasemsin, and Tosawat Seetawan, "The Effect of Temperature Sintering on Thermoelectric Property of Higher Manganese Silicide", ***Journal of Materials Science and Applied Energy.*** 6(3) (2017) 230 – 232 (ACI)
3. **K. Singsoog**, P. Pilasuta, S. Paengson, W. Namhongsa, S. Ruamruk, and T. Seetawan, Theoretical Thermoelectric Generator of n-Mg2Si and p-$MnSi_{1.75}$ Simulated by Finite Element Method, ***Materials today proceeding***, (Accepted) (Scopus)
4. **Kunchit Singsoog**, and Tosawat Seetawan, "Effecting the Thermoelectric Properties of p-$MnSi_{1.75}$ and n-$Mg_{1.98}Ag_{0.02}Si$ Module on Power Generation", ***Physica B***, (Revise)

K. Singsoog/ Journal of Materials Science and Applied Energy 6(1) (2017) 102–105

THE EFFECT OF SILVER AND BISMUTH DOPED Mg_2Si ON CRYSTAL STRUCTURE AND THERMOELECTRIC PROPERTIES

Kunchit Singsoog[a,b], Panida Pilasuta[a,b], Supasit Paengson[a,b], Wanachaporn Namhongsa[a,b], Weerasak Charoenrat[c], Surasak Ruamruk[a,b], Wiruj Impho[d], Phanuwat Wongsangnoi[d], Wasana Kasemsin[d], Tosawat Seetawan[a,b,*]

[a]*Thermoelectric Research Laboratory, Center of excellence on Alternative Energy, Research and Development Institute, Sakon Nakhon Rajabhat University, 680 Nittayo Road, Mueang District, Sakon Nakhon, 47000, Thailand.*
[b]*Program of Physics, Faculty of Science and Technology, Sakon Nakhon Rajabhat University, 680 Nittayo Road, Mueang District, Sakon Nakhon, 47000, Thailand.*
[c]*Program of Computer Science, Faculty of Science and Technology, Sakon Nakhon Rajabhat University, 680 Nittayo Road, Mueang District, Sakon Nakhon, 47000, Thailand.*
[d]*Faculty of Industrial Technology, Sakon Nakhon Rajabhat University, 680 Nittayo Road, Mueang District, Sakon Nakhon, 47000, Thailand.*

Received 27 December 2016; Revised 14 March 2017; Accepted 2 April 2017

ABSTRACT

Magnesium silicide have been high performance in temperature ranges 500 − 800 K which are medium-temperature and appropriate for applications with waste heat. The Ag and Bi doped Mg2Si were synthesized by hot press method. The crystal structure was analyzed by X-ray diffraction. Thermoelectric properties were measured in temperature rang 323 – 473 K. The XRD pattern of all samples show single crystal and crystallite size slightly increase for doped sample. The doped samples show thermal conductivity lower than un-dope and Ag-doped show maximum decrease about 44.44% at 473 K. The electrical resistivity of doped samples was decreased, and decrease 33% for Bi doped at 473 K. The doped materials slightly decreased Seebeck coefficient about 4% and 16% for Ag and Bi doped, respectively. The highest ZT was found in Ag doped about 0.47×10^{-2} at 473 K.

KEYWORDS: *Alternative Energy; Thermoelectric; Magnesium silicide; Silver; Bismuth*

* Corresponding authors; e-mail: t_seetawan@snru.ac.th

INTRODUCTION

Thermoelectric (TE) materials has been investigated in recent years for renewable heat energy into electricity. The performance of TE materials were confirmed by dimensionless figure of merit $ZT=S^2T/\sigma\kappa$, where S is Seebeck coefficient, T is temperature, σ is electrical resistivity and κ is thermal conductivity). Good TE materials needed to high Seebeck coefficient, low electrical resistivity and thermal conductivity. Magnesium silicide have been high performance in temperature ranges 500–800 K which are medium-temperature and appropriate for applications with waste heat. The highest ZT was reported about 1.4 for the $Mg_2(Si_{0.4}Sn_{0.6})Sb_{0.018}$ sample preparing by twice mechanical alloying and spark plasma sintering process [1], $Mg_2Si_{0.53}Sn_{0.4}Ge_{0.05}Bi_{0.02}$ preparing by solid state synthesis and sintering via hot pressing [2], $Mg_{2.16}(Si_{0.4}Sn_{0.6})_{0.97}Bi_{0.03}$ preparing by a two-step solid state reaction followed by spark plasma sintering. [3] and $Mg_2Si_{0.55}Sn_{0.4}Ge_{0.05}$:Bi=1:0.02 preparing by powder methods [4]. This research has objective for improve ZT of Mg_2Si by doped with Ag and Bi.

MATERIALS AND METHODS

The Ag and Bi doped Mg_2Si were prepared by solid state reaction and hot press method. Mg (99%, Aldrich), Si (99.9%, Aldrich), Ag (99.9%, Aldrich) and Bi (99%, Aldrich) were used as starting raw materials. The raw materials were mixed by ball milling for 12 h and calcined at

973 K for 1 h in Ar atmosphere. The powder placed in the graphite mold (ø20 mm) for hot press method at 1053 K under pressure 33 MPa for 1 h in Ar atmosphere.

The crystal structure was characterized by X-ray diffraction (XRD; Shimadzu 6100, Japan) method using CuKα radiation at 40 kV, 30 mA with a scanning speed of 5°/min at 2θ steps of 0.02°. The morphology was observed by scanning electron microscope (SEM; JEOL JSM–5401, Germany). Seebeck coefficient, electrical resistivity and thermal conductivity were measured by steady state method [5] at temperature ranges of 323 – 473 K.

RESULTS AND DISCUSSION

The X-ray diffraction analysis of Mg_2Si, $Mg_{1.98}Bi_{0.02}Si$ and $Mg_{1.98}Ag_{0.02}Si$ after hot press are compare with PDF#2 00-035-0773 as shown in Fig. 1. The crystal structure of all samples are show cubic Fm3m space group as a major phase, and the minor secondary phase MgO and Si are detected in all compositions due to the oxidation of Mg during the solid state reaction [6]. The SEM images magnification ×3500 show distribution, size and shape of particle. The particle size show 2–6 μm and evenly distribution as show in Fig. 2.

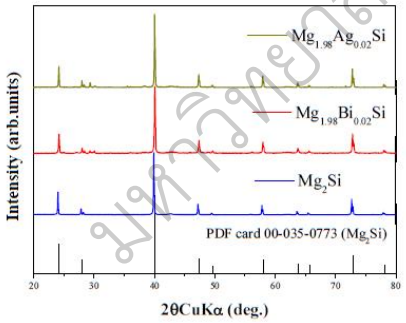

Fig. 1 XRD pattern of Mg_2Si (blue line) $Mg_{1.98}Bi_{0.02}Si$ (red line) and $Mg_{1.98}Ag_{0.02}Si$ (green line).

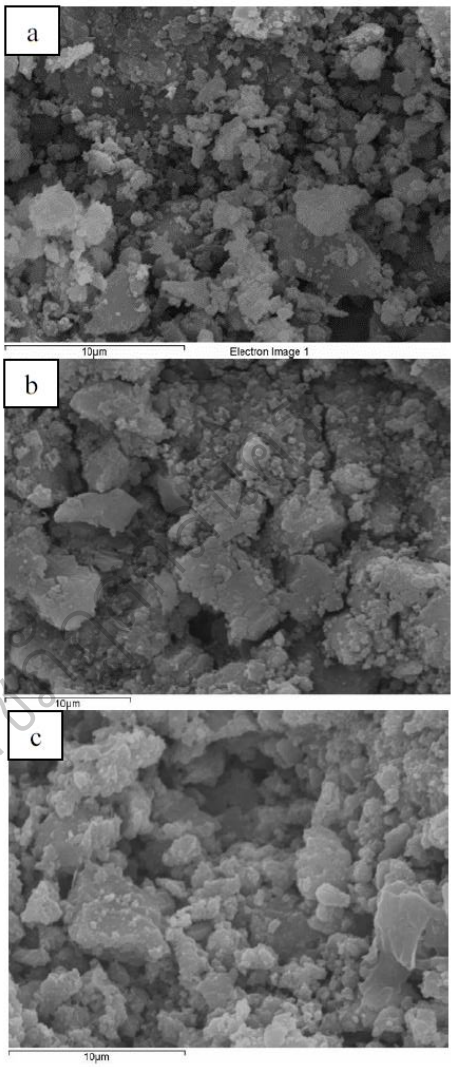

Fig. 2 SEM images of (a) Mg_2Si (b) $Mg_{1.98}Bi_{0.02}Si$ and (c) $Mg_{1.98}Ag_{0.02}Si$.

The Seebeck coefficient increases with temperature increasing but decreased when doping with Ag and Bi. The Mg_2Si shows highest value about −150 μV/K at 473 K as shown in Fig. 3.

Temperature dependence of electrical resistivity for Mg_2Si, $Mg_{1.98}Bi_{0.02}Si$ and $Mg_{1.98}Ag_{0.02}Si$ shows in Fig. 4. The Ag and Bi doped effect to decease electrical resistivity due to increase in carrier concentration and Bi doped shows lowest value about 60 mΩ cm at 473 K.

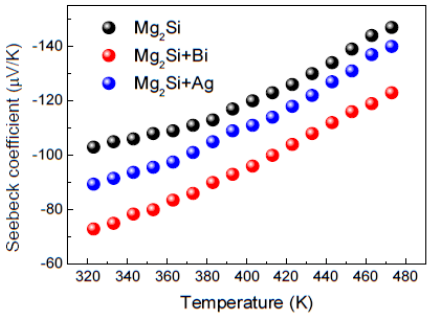

Fig. 3 Seebeck coefficient of Mg_2Si, $Mg_{1.98}Bi_{0.02}Si$ and $Mg_{1.98}Ag_{0.02}Si$ depend on temperature.

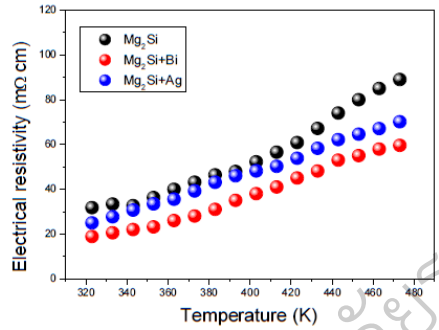

Fig. 4 Electrical resistivity of Mg_2Si, $Mg_{1.98}Bi_{0.02}Si$ and $Mg_{1.98}Ag_{0.02}Si$ depend on temperature.

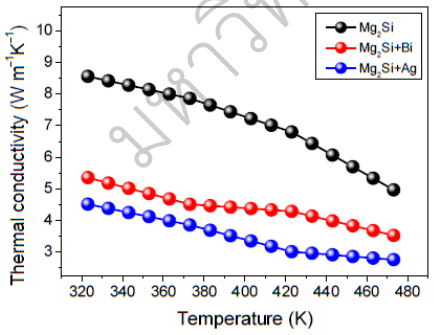

Fig. 5 Thermal conductivity of Mg_2Si, $Mg_{1.98}Bi_{0.02}Si$ and $Mg_{1.98}Ag_{0.02}Si$ depend on temperature.

Temperature dependence of thermal conductivity for Mg_2Si, $Mg_{1.98}Bi_{0.02}Si$ and $Mg_{1.98}Ag_{0.02}Si$ shows in Fig. 5. The doped samples can be decease thermal conductivity and Ag doped shows lowest thermal conductivity about 3 W/m K at 473 K as shown in Fig. 3 (c).

The Fig. 6 shows dimensionless figure of merit of Mg_2Si, $Mg_{1.98}Bi_{0.02}Si$ and $Mg_{1.98}Ag_{0.02}Si$. Doped samples show ZT value higher than un-dope and the Ag doped shows maximum ZT value about $0.47x10^{-2}$ at 473 K.

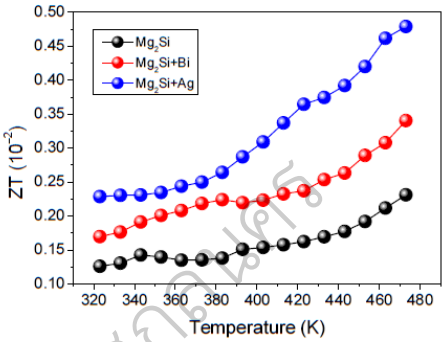

Fig. 6 Dimension less figure of merit of Mg_2Si, $Mg_{1.98}Bi_{0.02}Si$ and $Mg_{1.98}Ag_{0.02}Si$ depend on temperature.

CONCLUSION

The doped samples show thermal conductivity lower than un-dope and Ag doped show maximum decrease about 44.44% at 473 K. The electrical resistivity of doped samples was decreased, and decrease 33% for Bi doped at 473 K. The doped materials slightly decreased Seebeck coefficient about 4% and 16% for Ag and Bi doped, respectively. The highest ZT was found in Ag doped about 0.47×10^{-2} at 473 K.

REFERENCES

[1] L. Zheng, X. Zhang, H. Liu, S. Li, Z. Zhou, Q. Lu, J. Zhang, F. Zhang, Optimized nanostructure and thermoelectric performances of $Mg_2(Si_{0.4}Sn_{0.6})Sb_x$ solid solutions by in situ nanophase generation, J. Alloy. Compd. 671 (2016) 452–457.

[2] A.U. Khan, N.V. Vlachos, E. Hatzikraniotis, G.S. Polymeris, Ch.B. Lioutas, E.C. Stefanaki, K.M. Paraskevopoulos, I. Giapintzakis, Th. Kyratsi, Thermoelectric properties of highly efficient Bi-doped $Mg_2Si_{1-x-y}Sn_xGe_y$ materials, Acta Mater 77 (2014) 43–53.

[3] W. Liu, Q. Zhang, K. Yin, H. Chi, X. Zhou, X. Tang, C. Uher, High figure of merit and thermoelectric properties of Bi-doped $Mg_2Si_{0.4}Sn_{0.6}$ solid solutions, J. Solid. State. Chem. 203 (2013) 333–339.

[4] A.U. Khan, N. Vlachos and Th. Kyratsi, High thermoelectric figure of merit of $Mg_2Si_{0.55}Sn_{0.4}Ge_{0.05}$ materials doped with Bi and Sb, Scripta Mater. 69 (2013) 606–609.
[5] T. Sumphao, C. Thanachayanont, T. Seetawan, Design and Implementation of a Low Cost DAQ System for Thermoelectric Property Measurements, Procedia Eng. 32 (2012) 614 – 620.
[6] G. Kim, J. Kim, H. Lee, S. Cho, I. Lyo, S. Noh, B-W. Kim, S.W. Kim, K.H. Lee, W. Lee, Co-doping of Al and Bi to control the transport properties for improving thermoelectric performance of Mg_2Si, Scripta Mater. 116 (2016) 11–15.

K. Singsoog / Journal of Materials Science and Applied Energy 6(3) (2017) 230 – 232

The Effect of Sintering Temperature on Thermoelectric Property of Higher Manganese Silicide

Kunchit Singsoog [a, b,*], Panida Pilasuta [a, b], Supasit Paengson [a, b], Wanachaporn Namhongsa [a, b], Weerasak Charoenrat [c], Surasak Ruamruk [a, b], Phanuwat Wongsangnoi [d], Wiruj Impho [d], Wasana Kasemsin [d],

[a]*Thermoelectric Research Laboratory, Center of excellence on Alternative Energy, Research and Development Institute, Sakon Nakhon Rajabhat University, 680 Nittayo Road, Mueang District, Sakon Nakhon, 47000 Thailand*

[b]*Program of Physics, Faculty of Science and Technology, Sakon Nakhon Rajabhat University, 680 Nittayo Road, Mueang District, Sakon Nakhon, 47000 Thailand*

[c]*Program of Computer Science, Faculty of Science and Technology, Sakon Nakhon Rajabhat University, 680 Nittayo Road, Mueang District, Sakon Nakhon, 47000 Thailand*

[d]*Faculty of Industrial Technology, Sakon Nakhon Rajabhat University, 680 Nittayo Road, Mueang District, Sakon Nakhon, 47000 Thailand*

Received 30 October 2017; Revised 20 November 2017; Accepted 30 November 2017

Abstract

The Higher Manganese Silicide (HMS) was synthesized by solid state reaction and hot pressing. The various sintering temperature was started from 1123 K to 1223 K. The crystal structure and thermoelectric properties of samples were measured. The dimensionless figure of merit (ZT) was calculated from thermoelectric properties. The tetragonal structure of $MnSi_{1.75}$ was confirmed by X-ray diffraction (XRD). The Seebeck coefficient and Electrical resistivity are decreases, while the thermal conductivity increase when increasing sintering temperature. The maximum ZT of $MnSi_{1.75}$ was found in 1223 K of sintering temperature about 0.23 at 473 K.

KEYWORDS: Higher Manganese Silicide; Thermoelectric; Hot press

* Corresponding authors; e-mail: kunchitsingsoog@yahoo.com

Introduction

Thermoelectric materials have been used for alternative energy wherewith it can convert heat into electricity. However, the efficiency of thermoelectric material is limited for a wide variety of applications. The efficiency of the thermoelectric materials is defined by dimensionless figure of merit, $ZT = (S^2/\rho\kappa)T$, S is theSeebeck coefficient, ρ is the electrical resistivity, κ is thermal conductivities, and T is the absolute temperature. The Higher Manganese Silicide (HMS) was candidate for middle temperature of thermoelectric application due to the HMS showed high ZT in temperature ranges of 673 – 973 K. Recently, the undoped HMS was reported the ZT about 0.4 – 0.7 range by mechanical alloying and pulse discharge sintering [1], spark plasma sintering method [2, 3], hot press [4, 5], etc. In this work, has the objective for prepare the HMS by hot press method with various the sintering temperature from 1123 K to 1223 K to study the impact on thermoelectric properties.

Materials and Methods

The Higher Manganese Silicide was synthesized by solid state reaction and hot press method. Mn (99%, Aldrich) and Si (99.9%, Aldrich) were used raw materials. The raw materials were weighed in atomic ratio and mixed by ball milling for 2 h. The powder were placed in the alumina crucible and calcined in quartz tube furnace at 1073 K for 1 h in Ar atmosphere. The calcined powder were pressed in graphite mold (ø20 mm) and heated in temperature 1123 – 1223 K under pressure 33 MPa for 1 h in Ar atmosphere. The pellets were cut in size of $10\times10\times1$ mm^3 and $3\times3\times15$ mm^2 for crystal structure analysis and thermoelectric property measurement, respectively.

The X-ray diffraction (XRD; Shimadzu 6100, Japan) was used for crystal structure characterization. The CuKα radiation at 40 kV, 30

mA and a scanning speed of 5°/min at 2θ steps of 0.02° were setups for XRD condition. The thermoelectric properties include Seebeck coefficient, electrical resistivity and thermal conductivity were measured by steady state method [6] at temperature ranges of 323 – 473 K.

Results and Discussion

The powder XRD patterns of all samples are given in Fig. 1. The result of XRD show the main crystalline phase is $Mn_{27}Si_{47}$ with tetragonal structure (space group P - 4n2) and agree with PDF Number 00-026-1251. In addition, the common impurity phase MnSi was found for all sintering temperature. The 3×3×15 mm^3 HMS pellets were set up in the copper probe for Seebeck coefficient and electrical resistivity measurement and show the result in Fig. 2 and 3, respectively.

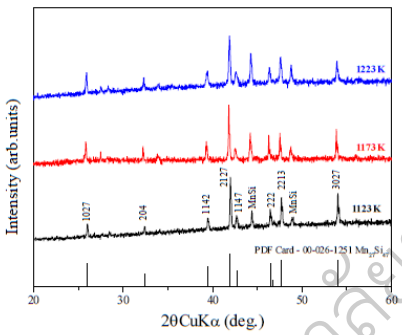

Fig. 1 XRD pattern of $MnSi_{1.75}$ as sintering temperature 1123 K, 1173 K and 1223 K

The Seebeck coefficient of all samples are positive value indicate that *p*-type thermoelectric material and decreases when sintering temperature increasing. The increase of S value with temperature indicate semiconductor behavior. The maximum of S value was found in 1123 K sintering sample about 201 μV K^{-1} at 473 K.

The higher sintering temperature can reduce electrical resistivity which the 1223 K sample shows the lowest value about 0.5 mΩ cm at 473 K. The electrical resistivity of all samples increases with temperature increase.

Fig. 4 shows the variation of the power factor ($S^2\rho$) in function of temperature for sintered samples. The power factor shows evolutions of the electrical conductivity and Seebeck coefficient in function of temperature. The 1123 K and 1173 K of sintering samples are small increases while 1223 K sintering sample shows the large increase with temperature. The maximum $S^2\rho$ = 3.02 mW m^{-1} K^{-2} is observed for the 1223 K sintering sample.

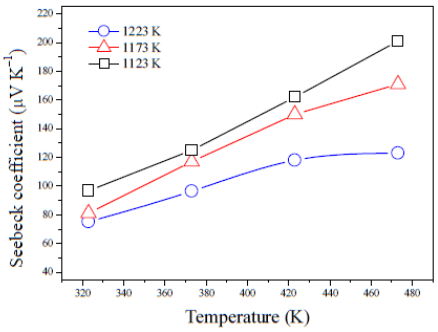

Fig. 2 Seebeck coefficient of $MnSi_{1.75}$ as sintering temperature 1123 K, 1173 K and 1223 K depend on temperature.

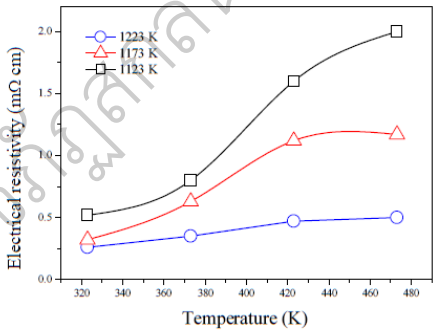

Fig. 3 Electrical resistivity of $MnSi_{1.75}$ as sintering temperature 1123 K, 1173 K and 1223 K depend on temperature

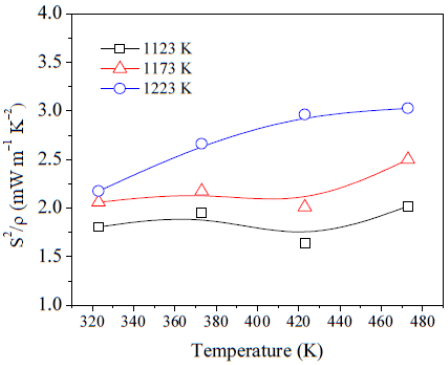

Fig. 4 The power factor of $MnSi_{1.75}$ as sintering temperature 1123 K, 1173 K and 1223 K depend on temperature

The thermal conductivity of sintered samples as a function of temperature is shown in Fig. 5. The thermal conductivity increases with sintering

temperature. The lowest κ = 4.79 Wm^{-1} K^{-1} is observed for the 1123 K sintering sample.

Fig. 6 shows the variation of the dimensionless figure of merit in function of temperature for sintered samples. The ZT of 1223 K sample shows the highest value about 0.23 at 473 K due to shows high S and low σ although highest κ.

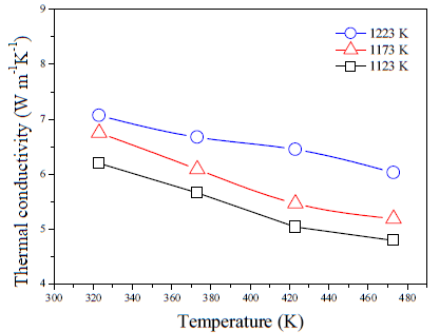

Fig. 5 Thermal coductivity of $MnSi_{1.75}$ as sintering temperature 1123 K, 1173 K and 1223 K depend on temperature

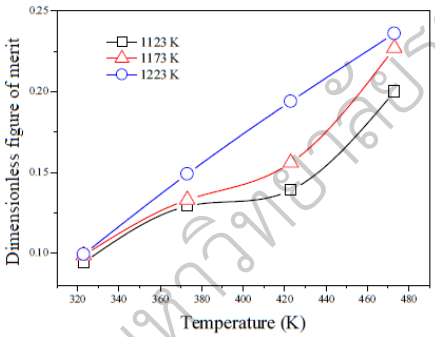

Fig. 6 Dimension less figure of merit of $MnSi_{1.75}$ as sintering temperature 1123 K (black line), 1173 K (red line) and 1223 K (blue line) depend on temperature

Conclusion

The synthesis of $MnSi_{1.75}$ was completed by hot press method. The various sintering temperature was affected to thermoelectric properties by means of high sintering temperature render to decrease S and ρ but increase κ. The maximum power factor is observed in 1223 K sintering sample about 3.02 mW m^{-1} K^{-2} at 473 K. The highest sintering temperature shows highest ZT about 0.23 at 473 K.

References

[1] T. Itoh, M. Yama, Synthesis of Thermoelectric Manganese Silicide by Mechanical Alloying and Pulse Discharge Sintering, J. Electron. Mater. 38(7) (2009) 925 – 929.

[2] W. Luo, H. Li, Y. Yan, Z. Lin, X. Tang, Q. Zhang, C. Uher, Rapid synthesis of high thermoelectric performance higher manganese silicide with in-situ formed nano-phase of MnSi, Intermetallics. 19 (2011) 404 – 408.

[3] G.B. Granger, M. Soulier, H.I. Mouko, C. Navone, M. Boidot, J. Leforestier, J. Simon, Microstructure investigations and thermoelectrical properties of a P-type polycrystalline higher manganese silicide material sintered from a gas-phase atomized powder, J. Alloy. Compd. 618 (2015) 403 – 412.

[4] D. Shin, K.Jang, S. Ur, I. Kim, Thermoelectric Properties of Higher Manganese Silicides Prepared by Mechanical Alloying and Hot Pressing, J. Electron. Mater. 42(7) (2013) 1756 – 1761.

[5] Y. Sadia, Z. Aminov, D. Mogilyansky, Y. Gelbstein, Texture anisotropy of higher manganese silicide following arc-melting and hot-pressing, Intermetallics. 68 (2016) 71 – 77.

[6] T. Sumphao , C. Thanachayanont, T. Seetawan, Design and Implementation of a Low Cost DAQ System for Thermoelectric Property Measurements, Procedia Engineering. 32 (2012) 614 – 620.

Available online at www.sciencedirect.com

ScienceDirect

Materials Today: Proceedings 00 (2018) 0000–0000

materialstoday: PROCEEDINGS

www.materialstoday.com/proceedings

MRS_2017

Theoretical Simulation of Thermoelectric Generator consisting of n-Mg_2Si and p-$MnSi_{1.75}$ by Finite Element Method

K. Singsoog[a,b], P. Pilasuta[a,b], S. Paengson[a,b], W. Namhongsa[a,b], S. Ruamruk[a,b], T. Seetawan [a,b]*

[a]*Thermoelectric Research Laboratory, Center of excellence on Alternative Energy, Research and Development Institute, Sakon Nakhon Rajabhat University, 680 Nittayo Road, Mueang District, Sakon Nakhon, 47000, Thailand*

[b]*Program of Physics, Faculty of Science and Technology, Sakon Nakhon Rajabhat University, 680 Nittayo Road, Mueang District, Sakon Nakhon, 47000, Thailand*

Abstract

We proposed the finite element (FEM) simulation model as an essential tool for understanding thermoelectric (TE) generator behavior. This model can predict the output power with various temperature difference, number and size of parameter conditions. It was found that the relationship between temperature difference and output power changed with volume of materials, number of cells and improved P-N connection design. The p-$MnSi_{1.75}$ and n-Mg_2Si thermoelectric module Model 2 obtained the maximum output power about 117 mW at a temperature difference of 200 K. This simulation model was applied to the optimization work on early designing stages of other material types on thermoelectric generators and coolers.

Selection and/or Peer-review under responsibility of The First Materials Research Society of Thailand International Conference.

Keywords: Numerical simulation, Generator, Thermoelectric materials, Magnesium silicide, Manganese silicide.

* Corresponding author. Tel.: +664-274-4319; fax: +664-274-4319.
E-mail address: t_seetawan@snru.ac.th

Selection and/or Peer-review under responsibility of The First Materials Research Society of Thailand International Conference.

1. Introduction

Thermoelectric technology is promoted for alternative energy development because the fact that it can convert heat into electricity [1]. The performance of thermoelectric material depends on the dimensionless figure of merit value ($ZT = S^2T / \rho_e\kappa$: S is Seebeck coefficient, T is absolute temperature, ρ_e is electrical resistivity and κ is thermal conductivity). Experimentally, the thermoelectric fabrication is difficult and time consuming due to many conditions involved. In theory, we can reduce time and resources by using the finite element method for prediction thermal properties and electric behavior of thermoelectric cell or module [2]. The main equation describing a system of thermoelectric including heat flow and continuity equations of electric charges as shown in Eq.(1) and (2) [3,4].

$$\rho_d C\frac{\partial T}{\partial t} + \vec{\nabla}\cdot\vec{q} = \dot{q} \tag{1}$$

where, ρ_d is density (k gm^{-3}), C is specific heat capacity (J kg^{-1} K^{-1}), $\vec{q}$ is heat flux vector (W m^{-2}) and $\dot{q}$ is heat generation rate per unit volume (W m^{-3}).

$$\vec{\nabla}\cdot\left(\vec{J} + \frac{\partial\vec{D}}{\partial t}\right) = 0 \tag{2}$$

where, $\vec{D}$ is electric flux density vector (C m^{-2}) and $\vec{J}$ is electric current density vector (A m^{-2}). Thermoelectric constitutive equation must be used as shown in Eq. (3).

$$\vec{q} = [\Pi]\cdot\vec{J} - [\lambda]\cdot\vec{\nabla}T \tag{3}$$

where, Π is Peltier coefficient matrix (V) and λ is thermal conductivity matrix (W m^{-}1 K^{-1}). The electrical current density is generated by Seebeck effect and Joule effect, as shown in Eq. (4).

$$\vec{J} = [\sigma]\cdot\vec{E} - [\sigma]\cdot[\alpha]\cdot\vec{\nabla}T \tag{4}$$

where, σ is electrical conductivity matrix (S m^{-1}) and α is Seebeck coefficient matrix (V K^{-1}). The constitutive equation for a dielectric medium is $\vec{D} = \varepsilon\cdot\vec{E}$, where ε is dielectric permittivity matrix. In the reduced of a time-variant magnetic field, the electric field is given by: $\vec{E} = -\vec{\nabla}\varphi$, where φ is an electric potential scalar. The constitutive equations of thermoelectricity are substituted Eq. (5) and (6).

$$\rho C\frac{\partial T}{\partial t} + \vec{\nabla}\left([\Pi]\cdot\vec{J}\right) - \vec{\nabla}\cdot\left([\lambda]\cdot\vec{\nabla}T\right) = \dot{q} \tag{5}$$

$$\vec{\nabla}\left([\varepsilon]\cdot\vec{\nabla}\frac{\partial\varphi}{\partial t}\right) + \vec{\nabla}\cdot\left([\sigma]\cdot[\alpha]\cdot\vec{\nabla}T\right) + \vec{\nabla}\cdot\left([\sigma]\cdot\vec{\nabla}\varphi\right) = 0 \tag{6}$$

2. Materials and Methods

The procedure of Galerkin FEM modified the thermoelectric equation into system of thermoelectric finite element equation [5,6]. The temperature and electric scalar potential over a finite element are approximated by $T = N\cdot T_e$ and $\varphi = N\cdot\vec{\varphi}_e$, where T_e is vector of nodal temperature, $\vec{\varphi}_e$ is vector of nodal electric potentials and N is vector of finite element shape functions. The resulting system of finite element equations can be written by Eq. (7),

$$\begin{bmatrix} C^{TT} & 0 \\ 0 & C^{\varphi\varphi} \end{bmatrix}\begin{pmatrix} \vec{T}_e \\ \vec{\varphi}_e \end{pmatrix} + \begin{bmatrix} K^{TT} & 0 \\ K^{\varphi T} & K^{\varphi\varphi} \end{bmatrix}\begin{pmatrix} \vec{T}_e \\ \vec{\varphi}_e \end{pmatrix} = \begin{pmatrix} \vec{Q} + \vec{Q}^P + \vec{Q}^e \\ I \end{pmatrix} \tag{7}$$

where C^{TT} is thermal damping matrix, $C^{\varphi\varphi}$ is dielectric damping matrix, K^{TT} is thermal stiffness matrix, $K^{\varphi T}$ is

Seebeck stiffness matrix, $K^{\varphi\varphi}$ is electric stiffness matrix, $\vec{Q}$ is vector of combined heat generation loads, $\vec{Q}^{P}$ is Peltier heat load vector and $\vec{Q}^{e}$ is electric power load vector.

The FEM simulation started from design thermoelectric leg, cell and TE module Model 1, 2 and 3 which the ingredient of TE is shown in Fig. 1. The materials properties are used in commercial software ANSYS as shown in Table 1 [7].

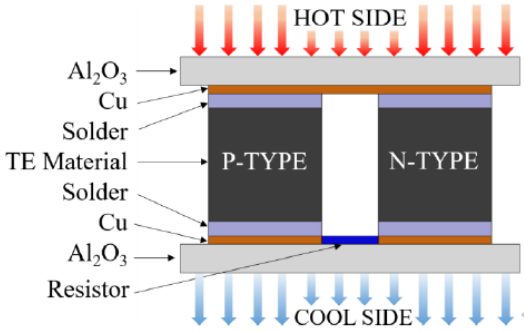

Fig. 1. The schematic diagram of thermoelectric cell design

Table 1. Materials properties at room temperature for thermoelectric module

Materials	S)μV K^{-1}(	ρ)Ω m(	κ)W m^{-1} K^{-1}(
$MnSi_{1.75}$	102.75	3.95×10^{-6}	6.71
Mg_2Si	−112.1	4.70×10^{-4}	3.53
Cu	-	1.7×10^{-6}	400
Solder	-	1.23×10^{-7}	55
Al_2O_3	-	-	35

Temperatures at hot side and cool side were set on both sides of TE module (T_h = 36 – 226 °C, T_c = 26 °C). The adjustable resistor was applied on electrode of P and N type for prediction the matching load resistance. The condition of voltage was set on electrode of N-type at 0 volt. The output power of TE legs and TE cell various sizes were simulated as a function of temperature difference. The TE module model 1, 2 and 3 designs are shown in Fig. 2.

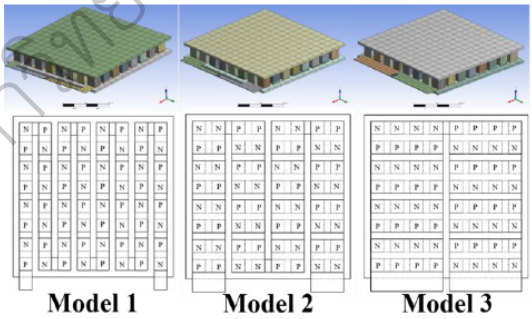

Fig. 2. The schematic diagram of TE module design

4. Results and Discussion

All authors are required to complete the license transfer agreement before the article can be published, which they can do online. This transfer agreement enables Elsevier to protect the copyrighted material for the authors, but does not relinquish the authors' proprietary rights. The copyright transfer covers the exclusive rights to reproduce and distribute the article, including reprints, photographic reproductions, microfilm or any other reproductions of similar nature and translations. Authors are responsible for obtaining from the copyright holder, the permission to reproduce any figures for which copyright exists.

4.1 $MnSi_{1.75}$ and Mg_2Si legs analysis

The $MnSi_{1.75}$ and Mg_2Si legs predicted the output power with different volume and temperature condition. The maximum output power is shown about 0.38 W by $MnSi_{1.75}$ leg size of 4×4×10 mm^3 at temperature difference of 200 K as shown in the Fig. 3 (a). The $MnSi_{1.75}$ has low electrical resistivity very close to output power with volume condition and cross section area. When the legs are higher, the output power is also increased as shown in Fig. 3 (a) and (b). The maximum output power of Mg_2Si at 8×8×6 mm^3 leg size is exhibited to be about 0.42 W as shown in Fig. 4 (a). The figure 4 (b) shows the relationship between cross section area and output power of Mg_2Si legs. The larger cross section area effected to higher output power. However, the output power is decreased, when the height of legs is increased.

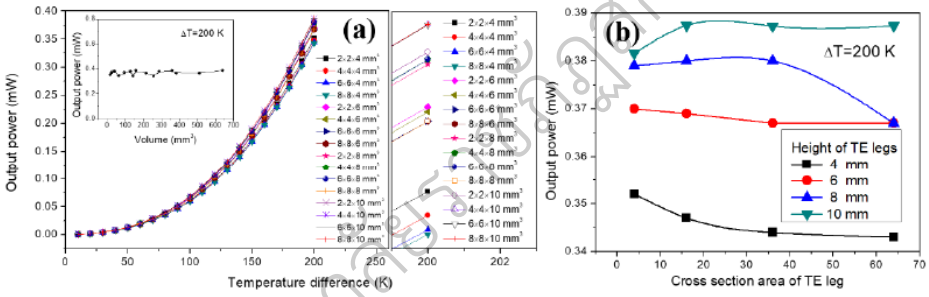

Fig. 3. The output power of $MnSi_{1.75}$ as a function (a) temperature difference and (b) cross section area

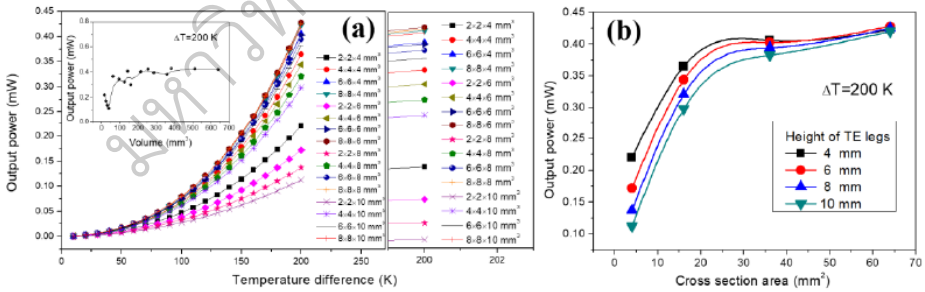

Fig. 4. The output power of Mg_2Si as a function of (a) temperature difference and (b) cross section area

4.2. TE cell analysis

The output powers were obtained from TE cells with different condition of cross section area of TE legs and temperature as shown in Fig. 5. This figure shows that the maximum output power of TE cell is about 0.80 W for P and N legs size 8×8×10 mm^3. However, the output power of volume condition for 4×4×10 mm^3 was compared with experimental data which it increased with increasing cross section area, as shown in Fig. 5.

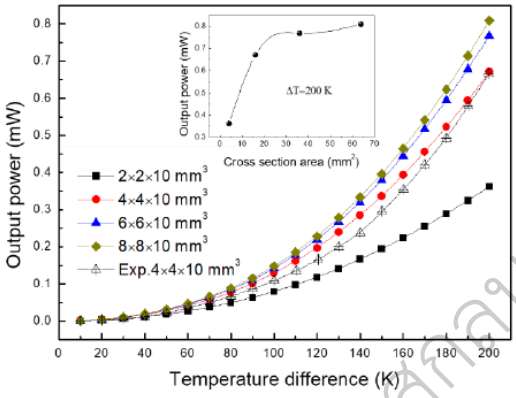

Fig. 5. The output power of TE cell as a function of temperature difference

The output powers were obtained from TE cells with different condition of height TE legs and temperature as shown in Fig. 6. This figure shows that the maximum output power of TE cell is about 0.72 W for p and n legs size 4×4×4 mm^3. In addition, the result of 4×4×10 mm^3 condition when compared with experimental data showed consistent value. When the height TE legs were increased, output power was decreased at temperature difference of 200 K as shown in Fig. 6.

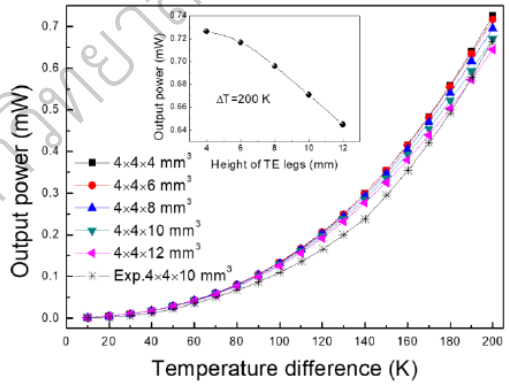

Fig. 6. The output power of TE cell as a function of temperature difference

4.3. TE module analysis

The relationships between output power as a function of electrical current and temperature difference of TE module Model 1, 2 and 3 are shown in the Fig.7 (a), (b), (c) and (d). The Matching load of TE module Model 1, 2 and 3 are 4 Ω, 0.8 Ω and 0.2 Ω respectively. In addition, the output power as a function of temperature of TE modules Model 1, 2 and 3 is shown in Fig. 7 (d). The Model 2 shows maximum output power about 117 mW at a temperature difference of 200 K indicate that the TE module of semiconductor materials are needed to connect by a mixed method between series and parallel to increase voltage and current.

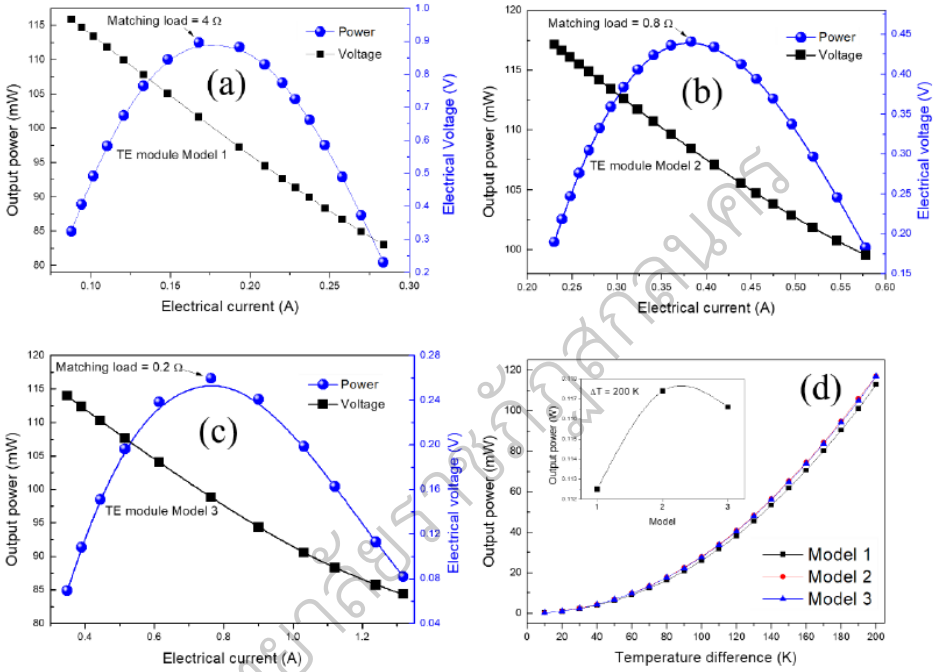

Fig. 7. The output power and electrical voltage as a function of electrical current of TE module (a) Model 1, (b) Model 2, (c) Model 3. (d) The output power of TE module as a function of temperature difference

5. Conclusions

The thermal and electric properties of TE legs, cell and module were simulated by finite element method. The output power of cell and module of p– and n– legs depended on different volume and electrical resistivity. The TE cell 4×4×4 mm^3 condition showed the best condition and good results. Therefore, we separated into three models; Model 1 showed maximum voltage, Model 2 showed maximum output power and Model 3 showed maximum current. However, we suggested the Model 2 showed maximum output power indicating that the TE module of semiconductor materials needed to connect by a mixed method between series and parallel for increasing voltage and current.

References

[1] K. Singsoog, C. Thanachayanont, A. Charoenphakdee, T. Seetawan, Key Eng Mater., 2016; 675-676: 679-682.
[2] E. E. Antonova, D. C. Looman,. In: ICT 2005 24th int conf thermoelectr., 2005; 200-3.
[3] T. Seetawana, U. Seetawan, A. Ratchasin, S. Srichai, K. Singsoog, W. Namhongsa, C. Ruttanapun, S. Siridejachai, Procedia Enginee., 2012;
[4] K. Singsoog, P. Pilasuta, S. Paengson, W. Namhongsa, W. Charoenrat, S. Ruamruk, W. Impho, P. Wongsangnoi, W. Kasemsin, T. Seetawan, J.Mater.Sci.Appl.Energ., 2017; (61): 102–105.
[5] N.S. Benday, D.M. Dryden, K. Kornbluth, P. Stroeve, Appl Energ., 2017;190:764–771.
[6] H. Hyland, H. Hunter, J. Liu, E. Veety, D. Vashaee, Appl Energ., 2016; 182: 518–24.
[7] T. Seetawan, K. Singsoog, S. Srichai, Adv Mat Res., 2013; 622-623: 220-223.